Angiogenesis and Vasculogenesis at 7-Day of Reperfused Acute Myocardial Infarction

Sheng Kang MD, PhD;[1] Yue-jin Yang MD;[2] Qing-zhi Wang MSc;[2] Yue Li MD, Yi Tian MD;[2] Yu-tong Cheng MD;[2] Wei-feng Shen MD, PhD[1]

1. Department of Cardiology, Rui Jin Hospital, Shanghai Jiaotong University School of Medicine, Rui Jin 2nd 197, Shanghai, 200025, People's Republic of China

2. Department of Cardiology, Cardiovascular Institute & Fu Wai Hospital, Chinese Academy of Medical Sciences & Peking Union Medical College, Bei Li Shi Rd 167, Beijing, 100037, China.

Abstract

Objectives

This study is to investigate the angiogenesis and vasculogenesis at the first week of reperfused acute myocardial infarction (AMI).

Methods

16 of mini-swines (20 to 30 Kg) were randomly assigned to the sham-operated group and the AMI group. The acute myocardial infarction and reperfusion model was created and the pig tail catheter was performed to monitor hemodynamics before left anterior descending coronary artery (LAD) occlusion, 90 min of LAD occlusion and 120 min of LAD reperfusion. Pathologic myocardial tissue was collected at 7-day of LAD reperfusion and further assessed by immunochemistry, dual immunochemistry, in-situ hybridization, real-time quantitative polymerase chain reaction and western blot.

Results

The infarcted area had higher FLK1 mRNA expression than sham-operated area and the normal area (all $P<0.05$), and the infarcted and marginal areas showed higher CD146 protein expression than the sham-operated area (all $P<0.05$), but the microvessel density (CD31 positive expression of microvessels/HP) was not significantly different between the infarcted area and the sham-operated area (8.92 ± 3.05 vs 6.43 ± 1.54) at 7-day of reperfused acute myocardial infarction ($P>0.05$).

Conclusions

FLK1 and CD146 expression significantly increase in the infarcted and marginal areas, and the microvessel density is not significantly different between the infarcted area and the sham-operated area, suggesting that angiogenesis and vasculogenesis in the infarcted area appear to high frequency of

increase in 7-day of reperfused myocardial infarction.

Introduction

Today salvaging the jeopardized myocardium is one of the most important clinical goals in acute myocardial infarction. However, after infarction, a repair process is initiated that strongly depends on vascular status. Rapid angiogenesis and residual vascular potency are important to the re-establishment of coronary collateral circulation and to the improvement of blood supply to the infarction zone and its periphery. FLK1, the tyrosine kinase receptor for vascular endothelial growth factor, is a marker for lateral plate mesoderm and the earliest differentiation marker for endothelial cells and blood cells[1] and FLK1 has been generally regarded as the major regulator of vasculogenesis (the recruitment of bone marrow-derived progenitors for endothelial cells)[2] and angiogenesis (the sprouting of preexisting vessels).[3,4]

Noticeably CD146 (Mel-CAM) is a ~118 kd member of the immunoglobulin superfamily of cell adhesion molecules[5] that was first recognized as a melanoma tumor progression antigen.[6-8] It is believed to be important for tumor cell–endothelium interaction.[9,10] CD146 joins VE-cadherin and CD31 (PECAM-1) as a molecule that mediates homotypic endothelial cell adhesion. CD146 has both structural functions and signaling functions important for endothelial monolayer integrity.[11]

On the other hand, CD31 is single strand glycoprotein distributed in cell membrane surface of endothelial cells, circulating platelets, monocytes, neutrophils, certain lymphocyte subsets, and megakaryocytic cell lines,[12,13] which used as endothelial marker in angiogenesis and vascularization investigation.[14-16]

To update, there is relatively little information regarding FLK1 and CD31, especially CD146 pattern of expression in case of reperfused acute myocardial infarction, thus we conducted a histopathology natural history study to investigate microvessel angiogenesis and vasculogenesis at 7-day of reperfused acute myocardium infarction.

Methods

Animal preparation

The animals and protocols used in the study were approved by the Institutional Animal Care and Use Committee. The mini-swines (20 to 30 Kg) were fasted overnight, sedated with 10 mg/kg of azaperone intramuscularly, anesthetized with 10 mg/kg of thiopental intravenously and ventilated with a respirator (Siemens elema sv 900, olna, Swede). Tidal volumes of 12 ml/kg with a set respiratory rate of 16 breaths per minute were used at first. Arterial PH, $PaCO_2$, and PaO_2 were monitored throughout the protocol by a blood gas analyzer (AGM-123-23, Finland) and maintained in a normal physiological range by adjusting the respiratory rate and/or tidal volume. Anesthesia was maintained with a continuous infusion of thiopental. A left lateral thoracotomy was performed, and the heart was suspended in a pericardial cradle.

The middle and distal portion of the left anterior descending coronary artery (LAD) was excised from surrounding tissue and was encircled by a suture. The two ends of the suture were threaded through a length of plastic tubing, forming a snare, which could be tightened to occlude the coronary artery. The right femoral artery were cannulated by 6 Fr pigtail guiding catheter for haemodynamic monitoring.

Sixteen animals were randomly assigned to eight sham-operated group and eight reperfused acute myocardial infarction group. The AMI and reperfusion model was created with 90 min of LAD occlusion followed by 7-day reperfusion. In the sham-operated animals, the LAD was only encircled by a suture, but not occluded. After the operation, the animals were sent to the observed room and were raised for 7 days, then were executed and we collected the relevant heart tissue.

Haemodynamic function

LAD occlusion was verified by ST segment elevation on the electrocardiogram. At baseline, at the end of 90 min of LAD occlusion and at 120 min of reperfusion, we measured heart rate (HR), left ventricular systolic pressure (LVSP), left ventricular end-diastolic pressure (LVEDP), the maximum change rate of left ventricular pressure rise and fall ($\pm dp/dt_{max}$).

Histopathological evaluation

After the completion of the experimental protocol, the swine was executed, the hearts were cut transversely and serially from the apex to the base (Figure 1). A slice obtained from the midpoint between the base and apex, which contained the greatest focus of myocardial infarction, was then cut from the myocardium in the three regions (the infarcted area, the marginal area and the normal area) in AMI group and healthy heart tissue (the sham-operated area) in the sham-operated group, washed thoroughly with saline and snap-frozen in liquid nitrogen or were fixed in 10% phosphate-buffered formalin (pH 7.35) and embedded in paraffin, cut into 4-μm sections, and affixed to glass slides for immunohistochemistry and in situ hybridization. (During all procedures, DEPC water and precaution against RNases were taken.)

In situ hybridization

First-strand cDNA synthesis was performed by the technicians in Beijing augct biotechnology company (Beijing, China). FLK1 cDNA sequence: AGATTACAGATCTCCATTTATTGCTTCTGTTAGTGACCA GCATGGAGTTGTGTACATCAC. After firststrand synthesis, cDNA was generated by PCR amplification with 10 pmol of specific primers for 30 cycles of amplification (94°C 1 s, 62°C 1 s, 72°C 1 s). cDNA probe labeling with digoxigenin-UTP by in vitro transcription with T7 RNA polymerase was performed as the manufacturer's instructions (DIG RNA labeling kit, SP6/T7, Boehringer Mannheim). Heart tissue was performed on 4-mm paraffin-embedded material sections using a nonradioactive in situ hybridization technique (Boehringer Mannheim). Using DEPC-treated equipment and solutions, paraffin-embedded specimens underwent sectioning, rehydration, and incubation in a prewarmed 5 ug/ml proteinase K solution.

Slides were then reimmersed in 4% PFA, treated with a 0.25% acetic anhydride, and dehydrated. Sections were exposed to a hybridization solution containing 50% formamide, 10% dextran sulfate, 1 mg/ml tRNA, 1×Denhardt's solution, 4×SSC, 50 mM Tris, and 5 mM EDTA that contained 20 ng/ul of DIG-labeled cDNA probe at 42°C overnight (10~12 hours). Slides were washed at 37°C in 2×SSC, 0.5×SSC, and 0.2×SSC twice for 15 min. After being rinsed with 0.2×SSC, DIG nucleic acid detection was accomplished using the Boehringer Mannheim. Slides underwent blocking in a 1% block reagent for 37℃ 30 min. Following blocking, slides were incubated with rabbit anti-DIG conjugate at 37°C 60 min, rinsed four times with 0.05 mmol/l PBS for 5 min each time, and similarly incubated goat anti-rabbit-AP IgG at 37°C 60 min, rinsed four times with 0.05 mmol/l PBS for 5 min each time, and then incubated with a dilute NBT/BCIP solution for 30min at 37℃. Slides were counterstained with a 0.1% nuclear fast red solution for 5 min, rinsed in water, air dried, and mounted. Hybridization without probe was performed as negative control and always showed no signals. All sections were examined and photographed under light microscopy.

Four hot spots of microvessel angiogenesis and vasculogenesis were searched in the stained sections under low power of light microscope (10×10), then computed the percentage of microvessel endothelial cells coated positive FLK1 mRNA expression divided by total microvessel endothelial cells under high power field (10×40) by the Leica Application Suite V2.3.4 R2 software (Leica Microsystems Ltd, Switzerland).

Immunohistochemistry

We randomly drew three samples from each group and employed primary antibody a mouse anti-human FLK1 antibody, secondary antibody polyclonal rabbit anti-mouse IgG (both from SANTA CRUZ BIOTECHNOLOGY, INC, U.S.A) for immunohistochemistry stain. Tissues were deparaffinized and underwent peroxide quenching. Using a histostain kit from Zhongshan Goldenbridge biotechnology Co (Beijing, China), after blocking, the sections were exposed to the primary antibody overnight at 4°C. Sections were then incubated with secondary biotinylated antibody as per the manufacturer's protocol. Horseradish peroxidase activity was visualized with a diaminobenzidine substrate and the sections were faintly counterstained with hematoxylin, and then observed under light microscope at 100× and 400× magnification.

Dual Immunohistochemistry

Dual immunohistochemistry was performed using peroxidase-based staining for smooth muscle actin simultaneously stained by alkaline phosphatase-based staining for CD31 developed with the polymer dual immunohistochemistry kit (Zhongshan Goldenbridge biotechnology Co, Beijing, China). Briefly, sections were pretreated with 3% hydrogen peroxide to inhibit endogenous peroxidase activity and incubated with 2% horse serum to block nonspecific protein binding. Subsequently, they were incubated with the primary antibody mouse anti-human α-smooth muscle actin and rabbit anti-human CD31(both from SANTA CRUZ BIOTECHNOLOGY, INC, U.S.A) for 10~12 hours at 4℃. After rinsing with PBS, the slides were

incubated for 30 min with the secondary antibody goat anti-mouse horseradish peroxidase IgG conjecture and goat anti-rabbit alkaline phosphatase IgG conjecture (both from Zhongshan Goldenbridge biotechnology Co, Beijing, China). The slides were rinsed with PBS and incubated for 30 min in ABC reagent.[17] Peroxidase activity was detected using diaminobenzidine with nickel (Vector). Slides were counterstained with hematoxylin. Sections incubated with PBS instead of primary antibody were used as negative controls. Angiogenesis endothelial cells marker CD31 ware stained into red color, and α-smooth muscle actin in vessel wall was stained into brown-yellow color. According to Weidner criterion:[18] single endothelial cell or endothelial cells' cluster marked with red color was defined as a microvessel, and excluded small artery with thick vascular smooth muscle and the luminal diameter beyond total 8 of red cells' diameters. Microvessel density (CD31 positive expression of microvessels/HP) measurement: firstly, 3 hot spots of angiogenesis and vasculogenesis were searched in the stained sections under low power of light microscope (10×10), then compute average of microvessels coated with CD31 positive endothelial cells under 4 of high power field (HP:10×40) by the Leica Application Suite V2.3.4 R2 software (Leica Microsystems Ltd, Switzerland).

Tissue preparation and RNA isolation

We randomly sampled 6 of specimen from each group (the sham-operated area, the infarcted area, the marginal area and the normal area) for Real-time Quantitative Polymerase Chain Reaction (RQ-PCR). A piece of frozen tissue (0.1– 0.5 g) was grinded in liquid nitrogen. Total RNA was prepared immediately with Trizol reagent, according to the manufacturer's protocol using Trizol (Invitrogen Life Technologies, Carslbad, CA). Briefly, a piece of frozen tissue (50~100mg) were homogenized with 1~2 ml of Trizol, after which 400 ul of chloroform was added and the mixture was shaken vigorously, followed by centrifugation at 12 000 rpm for 15 min. Total RNA was precipitated by isopropyl alcohol and then dissolved with 30~35 ul of RNase-free water.

Real-time Quantitative Polymerase Chain Reaction (RQ-PCR)

A RQ-PCR method was used for detection of FLK1 mRNA expression. The RT-PCR kit (Invitrogen Life Technologies Co, U.S.A) and the ABI PRISM 7700 Sequence Detector (ABI Co, U.S.A) were used according to the manufacturer's protocol. β-specific mRNA was used for standardization. Each sample was detected in thrice. Standard curves had a correlation coefficient of > 0.998. The specific RNA was determined in the different heart tissue (the sham-operated area, the infarcted area, the marginal area and the normal area) from 1ug of total RNA to be reversed and transcribed into cDNA using a SuperScriptw first-strand synthesis system for RT-PCR (Invitrogen Life Technologies Co, U.S.A). The first strand cDNA was amplified using Taq polymerase (Takara, Shiga, Japan). Sybr Green I (10×) was used for label (Invitrogen Life Technologies Co, U.S.A). The oligonucleotide primer sequences used for the PCR reactions were indicated as following. The presence of corresponding PCR products was verified by electrophoresis on a 2% agarose gel in 1x Tris–acetate– EDTA buffer.

PCR reagent formulation:

cDNA	2ul
dNTPs (10mM)	0.5ul
10×PCR buffer	2.5ul
primer f (20pmol/ul)	0.25ul
primer r (20pmol/ul)	0.25ul
Taq DNA polymerase mixture	0.2ul
Sybr Green I (10×)	1ul
ddH_2O	(add ddH_2O to total volume 25ul)

RQ-PCR condition:

(1) β-actin:

Cycle time: 90 Seconds;

94℃ predenaturalization for 2 min;

94℃ denaturalization for 150 sec;

72℃ annealing and extension for 30/30 sec;

CT: 35 cycles;

Primer F 5'→3' ATCATGTTTGAGACCTTC AACA;

Primer R 5'→3' CATCTCTTGCTCGAAGTCCA;

PCR production: 318 bp.

(2) FLK1:

Cycle time: 60 Seconds;

94℃ predenaturalization for 2 min;

94℃ denaturalization for 150 sec;

72℃ annealing and extension for 30/30 sec;

CT: 35 cycles;

Primer F 5'→3' TGATCGGAA ATGACACTGGA;

Primer R 5'→3' TTCTGGATACCTCGCACAAA;

PCR production: 224 bp.

Western blot analysis for CD146 in heart tissue

The heart biopsy specimens was washed by physiological saline and frozen at −70 °C until use. Protein concentration was determined by the method of Bradford.[19] 100 μg of total protein solubilized for 10 min at 100 °C was loaded per lane onto a 10% SDSPAGE gel. Electrophoresis was performed for 40~60 min at 120 v. Proteins were transferred onto immobilon-P transfer membrane (Millipore, Bedford, MA, U.S.A.) for 1.5~3 h at 0.8 mA/cm^2 in a 20% methanol containing cathodes buffer. The membrane was washed in

PBST (0.1% Tween 20, 100 mM Tris–HCL, 150 mM NaCl, pH 7.5), blocked for 1 h in 5% nonfat milk-TBST (pH 7.2 Tris-buffered saline containing 0.05% Tween 20) and incubated with 1:300 dilution of goat anti-human polyclonal antibodies CD146 (from Santa Cruz Biotechnology Inc, U.S.A). After being washed, the membrane was incubated with a 1:5000 dilution of the rabbit anti-goat secondary antibody (Sigma-Aldrich Co, U.S.A) for 30 min at room temperature. To express the tested proteins relative to actin, membranes were reblotted with anti-actin antibody, and relative intensities of protein and β-actin calculated. β-actin protein expression served as an internal control. For quantification, Western blot gels were scanned and bands quantified by integrating intensity and area using a commercial computer program (Alphalmager^{TM} IS-3400 V. 4.0.1, Alpha Innotech, U.S.A).

Statistical methods

Data was evaluated for normality of distribution. Comparisons of data among all stages were performed with one-way ANOVA followed by the Newman-Keuls multiple comparison test. The nonparametric Mann-Whitney U test was used in skew data. The proportion was analyzed by Chi-square test. All statistical analyses were performed with SPSS for windows (version 10.0, Chicago). A value of $P<0.05$ (2-sided) was considered statistically significant.

Result

Compared with the sham-operated group, the AMI group had higher dp/dt_{max} (3048.57±564.37 vs 2335.88 ±623.48, P=0.038) in left ventricle before the LAD was occluded (Table 1), but not significant difference between the two groups in other variables including weight, male (%), heart rate, systolic and diastolic aortic pressure, LVSP, LVEDP and $-dp/dt_{max}$.

In situ hybridization detection, the infarcted and marginal areas had higher the positive rate of FLK1 mRNA expression compared with the normal area and the sham-operated area ($P<0.05$), and so were the infarcted area vs. the marginal area ($P<0.05$) (Figure 2).

In RQ-PCR analysis, the infarcted area showed significantly higher the FLK1 mRNA expression compared with the normal area and the sham-operated area ($P<0.05$) (Figure 3)

According to immunohistochemical staining, the FLK1 protein expression was found in the infarcted area but not in the marginal area, the normal area and the sham-operated area (Figure 4).

In Western blot analysis, the infarcted and marginal areas had higher the CD146 protein expression compared with the normal area and the sham-operated area ($P<0.05$) (Figure 5).

Using dual immunohistochemical staining, we found that the microvessel density (CD31 positive expression of microvessels/HP) between the infarcted area and the sham-operated area was not statistically significant (8.92±3.05 vs 6.43±1.54) at 7-day of reperfused acute myocardial infarction ($P>0.05$) (Figure 6).

Discussion

In 7-day of reperfused acute myocardial infarction, the present study found (1) the infarcted area had higher FLK1 mRNA expression than sham-operated area and the normal area; (2) the infarcted area also showed higher CD146 protein expression than the sham-operated area; (3) the microvessel density was not significantly different between the infarcted area and the sham-operated area, suggesting angiogenesis and vasculogenesis in the infarcted area appear to high frequency of increase in the infarcted area.

Vessel growth and maturation are critical for scar formation and cardiac repair. This process represents an important therapeutic target in our efforts to improve post-infarction cardiac recovery.[20,21] Infarct microvessels undergo phenotypic changes and, after an initial phase of plasticity associated with intense angiogenic activity to meet the metabolic needs of the cellular scar, pericyte recruitment may mark the creation of a more mature vasculature.[22]

Angiogenic endothelial cells demonstrate phenotypic characteristics distinctly different from those of resting quiescent endothelial cells. Sprouting neovessels have been shown to express the integrins αvβ3 [23,24] and αvβ5,[25] the cell surface glycoprotein Thy-1,[26] and the VEGF receptor FLK1/kDR,[27] whereas proliferating endothelial cells demonstrate increased expression of adhesion molecules such as E-selectin.[28]

The knockout studies show that homozygous disruption of FLK1 gene leads to early embryonic death due to a failure of vasculogenesis, whereas homozygous Flt1 disruption allows normal vascular endothelial differentiation and development but leads to a failure to assemble normal vascular channels.[29,30]

Ischemia induced VEGF and its receptors (FLK1 and Flt1) upregulation, and increase angiogenesis and vasculogenesis in ischemic myocardium.[31] In situ hybridization, only endothelial cells were expressing these receptors. Another unexpected observation was the finding that while Flt1 was expressed in endothelium of both large and small vessels, FLK1 expression was restricted to small (<l00 mm in diameter) vessels, and the increased VEGF, FLK1 and Flt1 mRNA expression in the left ventricular myocardium as early as 1 h after LAD ligation in the rat, furthermore, by 7 days and as late as 6 wk, elevated expression of mRNA of FLK1 and Flt1 was confined to the infarct zone.[32] Similarly we also found that there was increased positive rate of FLK1 mRNA expression by the viable endothelial cells in the infarcted area at 7-day of LAD reperfusion, and only FLK1 protein expression was found in the infarcted area by immunohistochemistry stain.

CD146 is a transmembrane glycoprotein constitutively expressed on endothelial cells,[33,34] with a potential role in cell adhesion and in the rearrangement of the actin cytoskeleton.[35] Infarct microvessels showed CD146 immunoreactivity in all stages of healing. Although biologic functions have been ascribed to CD146 expression on various cell types, very little is known about the biologic role of CD146 on

endothelial cells. Endothelial CD146 is found to support homotypic cell to cell adhesions that are important in maintaining blood vessel integrity and in controlling intercellular permeability.[36,37] The ability of endothelial cells to form heterotypic CD146-dependent adhesions may be important in transendothelial migration or even hemangioblast differentiation.[11]

Late studies found that CD146 showed specific overexpression in angiogenesis and vasculogenesis process,[38] for example, the infarct endothelial cells in the early phase of healing showed intense staining for CD31 and CD146,[22] which was consistent with our findings that the infarcted area showed higher CD146 protein expression compared with the sham-operated area ($P<0.05$).

Platelet/endothelial cell adhesion molecule-1 (CD31) is a 130-kD member of the immunoglobulin gene superfamily whose expression is restricted exclusively to certain cells of the vasculature.[39,40] On endothelial cells, CD31 is expressed constitutively at $1x10^6$ molecules per cell, making CD31 the most highly expressed adhesion molecule on the endothelial cell surface.[12]

Healing MIs contain a large number of capillaries in the early stages of healing.[41] Scar maturation was associated with the increasing presence of pericyte-coated vessels in the infarcted region. In the early stages of healing (7 days of reperfusion), significant numbers of microvessels without an α-smooth muscle actin-positive pericyte coat were noted.[22] Similarly our study suggested that the microvessel density (CD31 positive expression of microvessels/HP) was slightly higher in the infarcted area compared with the sham-operated area (8.92±3.05 vs 6.43±1.54, $P>0.05$), thus we speculate that angiogenesis and vasculogenesis in the infarcted area appear to high frequency of increase in 7-day of reperfused myocardial infarction.

Limitation (1) we did not elucidate the mechanism of microvessel angiogenesis and vasculogenesis influence on left ventricle remodeling in the salvaged myocardial tissue at 7-day of reperfused myocardial infarction. (2) angiogenesis and vasculogenesis are a very complex process, and methods are available for demonstrating the wide range of gene products involved at all its stages. Further examinations of VEGF, Flt1 and circulating endothelial progenitor cells are warranted.

Conclusion

FLK1 and CD146 expression significantly increase in the infarcted and marginal areas, and the microvessel density is not significantly different between the infarcted area and the sham-operated area, suggesting that angiogenesis and vasculogenesis in the infarcted area appear to high frequency of increase in 7-day of reperfused myocardial infarction.

Acknowledgement

We sincerely thank those technicians: Ying-zi Xiao provided us with in situ hybridization technique support; Xiao-le Zhu provided us with real-time quantitative PCR technique support and Chong Xu provided us with Western blot technique support. We would also like to very thank the staff in the department of experiment surgery and the department of pathology (Fu Wai hospital, Beijing, China) for providing us with relevant technique support. This work was supported by a grant from national important basic research development of 973 project, People's Republic of China (Number: 2005CB523303).

Reference

1. Kabrun N, Bühring HJ, Choi K, Ullrich A, Risau W, Keller G. Flk-1 expression defines a population of early embryonic hematopoietic precursors. Development. 1997;124(10):2039-48.
2. Asahara T, Murohara T, Sullivan A, Silver M, van der Zee R, Li T, Witzenbichler B, Schatteman G, Isner JM. Isolation of putative progenitor endothelial cells for angiogenesis. Science. 1997; 275 (5302): 964-7.
3. Folkman J. Angiogenesis in cancer, vascular, rheumatoid and other disease. Nat Med. 1995; 1(1): 27-31.
4. Tille JC, Wang X, Lipson KE, McMahon G, Ferrara N, Zhu Z, Hicklin DJ, Sleeman JP, Eriksson U, Alitalo K, Pepper MS. Vascular endothelial growth factor (VEGF) receptor-2 signaling mediates VEGF-C(deltaNdeltaC)- and VEGF-A-induced angiogenesis in vitro. Exp Cell Res. 2003; 285(2): 286-98.
5. Lehmann JM, Riethmüller G, Johnson JP. MUC18, a marker of tumor progression in human melanoma, shows sequence similarity to the neural cell adhesion molecules of the immunoglobulin superfamily. Proc Natl Acad Sci U S A. 1989;86(24):9891-5.
6. Johnson JP, Rummel MM, Rothbächer U, Sers C. MUC18: A cell adhesion molecule with a potential role in tumor growth and tumor cell dissemination. Curr Top Microbiol Immunol. 1996;213 (Pt 1):95-105.
7. Sers C, Riethmüller G, Johnson JP. MUC18, a melanoma-progression associated molecule, and its potential role in tumor vascularization and hematogenous spread. Cancer Res. 1994; 54(21): 5689 -94.
8. Johnson JP, Lehmann JM, Stade BG, Rothbächer U, Sers C, Riethmüller G. Functional aspects of three molecules associated with metastasis development in human malignant melanoma. Invasion Metastasis. 1989;9(6):338-50.
9. Xie S, Luca M, Huang S, Gutman M, Reich R, Johnson JP, Bar-Eli M. Expression of MCAM/MUC18 by human melanoma cells leads to increased tumor growth and metastasis. Cancer Res. 1997;57(11): 2295-303.
10. Shih IM, Speicher D, Hsu MY, Levine E, Herlyn M. Melanoma cell-cell interactions are mediated through heterophilic Mel-CAM/ligand adhesion. Cancer Res. 1997;57(17):3835-40.
11. Solovey AN, Gui L, Chang L, Enenstein J, Browne PV, Hebbel RP. Identification and functional assessment of endothelial P1H12. J Lab Clin Med. 2001;138(5):322-31.
12. Newman PJ. The role of PECAM-1 in vascular cell biology. Ann N Y Acad Sci. 1994;714:165-74.
13. DeLisser HM, Newman PJ, Albelda SM. Molecular and functional aspects of PECAM-1/CD31. Immunol Today. 1994;15(10):490-5.
14. Sheibani N, Frazier WA. Thrombospondin-1, PECAM-1, and regulation of angiogenesis. Histol Histopathol. 1999;14(1):285-94.
15. Bruno S, Bussolati B, Scacciatella P, Marra S, Sanavio F, Tarella C, Camussi G. Combined administration of G-CSF and GM-CSF stimulates monocyte-derived pro-angiogenic cells in patients

with acute myocardial infarction. Cytokine. 2006;34(1-2):56-65.

16. Numaguchi Y, Sone T, Okumura K, Ishii M, Morita Y, Kubota R, Yokouchi K, Imai H, Harada M, Osanai H, Kondo T, Murohara T. The impact of the capability of circulating progenitor cell to differentiate on myocardial salvage in patients with primary acute myocardial infarction. Circulation. 2006;114(1 Suppl):I114-9.
17. Hsu SM, Raine L, Fanger H. Use of avidin-biotin-peroxidase complex (ABC) in immunoperoxidase techniques: a comparison between ABC and unlabeled antibody (PAP) procedures. J Histochem Cytochem. 1981;29(4):577-80.
18. Folkman J. Angiogenesis in cancer, vascular, rheumatoid and other disease. Nat Med. 1995; 1(1): 27-31.
19. Bradford MM. A rapid and sensitive method for the quantitation of microgram quantities of protein utilizing the principle of protein-dye binding. Anal Biochem. 1976;72:248-54.
20. Heymans S, Luttun A, Nuyens D, Theilmeier G, Creemers E, Moons L, Dyspersin GD, Cleutjens JP, Shipley M, Angellilo A, Levi M, Nübe O, Baker A, Keshet E, Lupu F, Herbert JM, Smits JF, Shapiro SD, Baes M, Borgers M, Collen D, Daemen MJ, Carmeliet P. Inhibition of plasminogen activators or matrix metalloproteinases prevents cardiac rupture but impairs therapeutic angiogenesis and causes cardiac failure. Nat Med. 1999;5(10):1135-42.
21. Carmeliet P. Mechanisms of angiogenesis and arteriogenesis. Nat Med. 2000;6(4):389-95.
22. Ren G, Michael LH, Entman ML, Frangogiannis NG.. Morphological characteristics of the microvasculature in healing myocardial infarcts. J Histochem Cytochem. 2002 Jan;50(1):71-9.
23. Brooks PC, Clark RA, Cheresh DA. Requirement of vascular integrin alpha v beta 3 for angiogenesis. Science. 1994;264(5158):569-71.
24. Clark RA, Tonnesen MG, Gailit J, Cheresh DA. Transient functional expression of alphaVbeta 3 on vascular cells during wound repair. Am J Pathol. 1996;148(5):1407-21.
25. Friedlander M, Theesfeld CL, Sugita M, Fruttiger M, Thomas MA, Chang S, Cheresh DA. Involvement of integrins alpha v beta 3 and alpha v beta 5 in ocular neovascular diseases. Proc Natl Acad Sci U S A. 1996;93(18):9764-9.
26. Lee WS, Jain MK, Arkonac BM, Zhang D, Shaw SY, Kashiki S, Maemura K, Lee SL, Hollenberg NK, Lee ME, Haber E. Thy-1, a novel marker for angiogenesis upregulated by inflammatory cytokines. Circ Res. 1998;82(8):845-51.
27. Millauer B, Wizigmann-Voos S, Schnürch H, Martinez R, Møller NP, Risau W, Ullrich A. High affinity VEGF binding and developmental expression suggest Flk-1 as a major regulator of vasculogenesis and angiogenesis. Cell. 1993;72(6):835-46.
28. Bischoff J, Brasel C, Kräling B, Vranovska K. E-selectin is upregulated in proliferating endothelial cells in vitro. Microcirculation. 1997;4(2):279-87.
29. Fong GH, Rossant J, Gertsenstein M, Breitman ML. Role of the Flt-1 receptor tyrosine kinase in regulating the assembly of vascular endothelium. Nature. 1995;376(6535):66-70.

30. Sharma HS, Wünsch M, Schmidt M, Schott RJ, Kandolf R, Schaper W. Expression of angiogenic growth factors in the collateralized swine myocardium. EXS. 1992;61:255-60.
31. Schultz A, Lavie L, Hochberg I, Beyar R, Stone T, Skorecki K, Lavie P, Roguin A, Levy AP. Interindividual heterogeneity in the hypoxic regulation of VEGF: significance for the development of the coronary artery collateral circulation. Circulation. 1999;100(5): 547-52.
32. Li J, Brown LF, Hibberd MG, Grossman JD, Morgan JP, Simons M. VEGF, flk-1, and flt-1 expression in a rat myocardial infarction model of angiogenesis. Am J Physiol. 1996;270(5 Pt 2): H1803-11.
33. Bardin N, Francès V, Lesaule G, Horschowski N, George F, Sampol J. Identification of the S-Endo 1 endothelial-associated antigen. Biochem Biophys Res Commun. 1996;218(1):210-6.
34. Shih IM. The role of CD146 (Mel-CAM) in biology and pathology. J Pathol. 1999;189(1):4-11.
35. Anfosso F, Bardin N, Vivier E, Sabatier F, Sampol J, Dignat-George F. Outside-in signaling pathway linked to CD146 engagement in human endothelial cells. J Biol Chem. 2001;276(2): 1564-9.
36. Bardin N, George F, Mutin M, Brisson C, Horschowski N, Francés V, Lesaule G, Sampol J. S-Endo 1, a pan-endothelial monoclonal antibody recognizing a novel human endothelial antigen. Tissue Antigens. 1996;48(5):531-9.
37. Shih IM, Elder DE, Speicher D, Johnson JP, Herlyn M. Isolation and functional characterization of the A32 melanoma-associated antigen.Cancer Res. 1994;54(9):2514-20.
38. Melnikova VO, Bar-Eli M. Bioimmunotherapy for melanoma using fully human antibodies targeting MCAM/MUC18 and IL-8. Pigment Cell Res. 2006;19(5):395-405.
39. Newman PJ, Berndt MC, Gorski J, White GC 2nd, Lyman S, Paddock C, Muller WA. PECAM-1 (CD31) cloning and relation to adhesion molecules of the immunoglobulin gene superfamily. Science. 1990;247(4947):1219-22.
40. Albelda SM, Muller WA, Buck CA, Newman PJ. Molecular and cellular properties of PECAM-1 (endoCAM/CD31): a novel vascular cell-cell adhesion molecule. J Cell Biol. 1991;114(5):1059- 68.
41. Frangogiannis NG, Michael LH, Entman ML. Myofibroblasts in reperfused myocardial infarcts express the embryonic form of smooth muscle myosin heavy chain (SMemb). Cardiovasc Res. 2000; 48(1):89-100.

Table 1. General and hemodynamics characteristics in the reperfused myocardial infarction model.

	Sham-operated group (N = 8)	AMI group (N = 8)	P value
Weight (kg)	19.39±2.75	22.04±2.35	0.065
Gender (male, %)	42.9	50.0	0.782
Heart Rate (beats/min)			
Baseline	113.63±29.14	108.88±23.46	0.725
Ischaemic 90 min	112.14±22.70	117.71±27.34	0.686
Reperfusion 120 min	109.00±31.86	110.00±27.85	0.948
Systolic aortic pressure (mm Hg)			
Baseline	108.00±18.99	110.94±31.05	0.822
Ischaemic 90 min	103.09±19.13	99.59±18.52	0.734
Reperfusion 120 min	98.45±24.83	92.75±30.38	0.707
Diastolic aortic pressure (mm Hg)			
Baseline	75.59±26.73	82.05±24.79	0.624
Ischaemic 90 min	76.36±16.84	76.70±13.19	0.967
Reperfusion 120 min	73.74±27.04	65.35±19.96	0.521
LVSP (mm Hg)			
Baseline	111.62±19.15	112.14±27.44	0.966
Reperfusion 120 min	102.38±21.55	87.76±25.70	0.258
LVEDP (mm Hg)			
Baseline	1.14±5.88	-1.96±5.97	0.330
Reperfusion 120 min	-0.21±6.60	-0.54±5.46	0.918
$+dp/dt_{max}$ (mm Hg/s)			
Baseline	2335.88±623.48	3048.57±564.37	0.038
Reperfusion 120 min	2036.57±635.09	1883.75±606.02	0.642
$-dp/dt_{max}$ (mm Hg/s)			
Baseline	-1528.88±535.42	-1591.43±274.19	0.785
Reperfusion 120 min	-1548.43±655.85	-1262.50±696.29	0.430

Note: Note: data was described as mean±SD or proportion. LVSP, left ventricular systolic pressure; LVEDP, left ventricular end-diastolic pressure; $\pm dp/dt_{max}$, the maximum change rate of left ventricular pressure rise and fall.

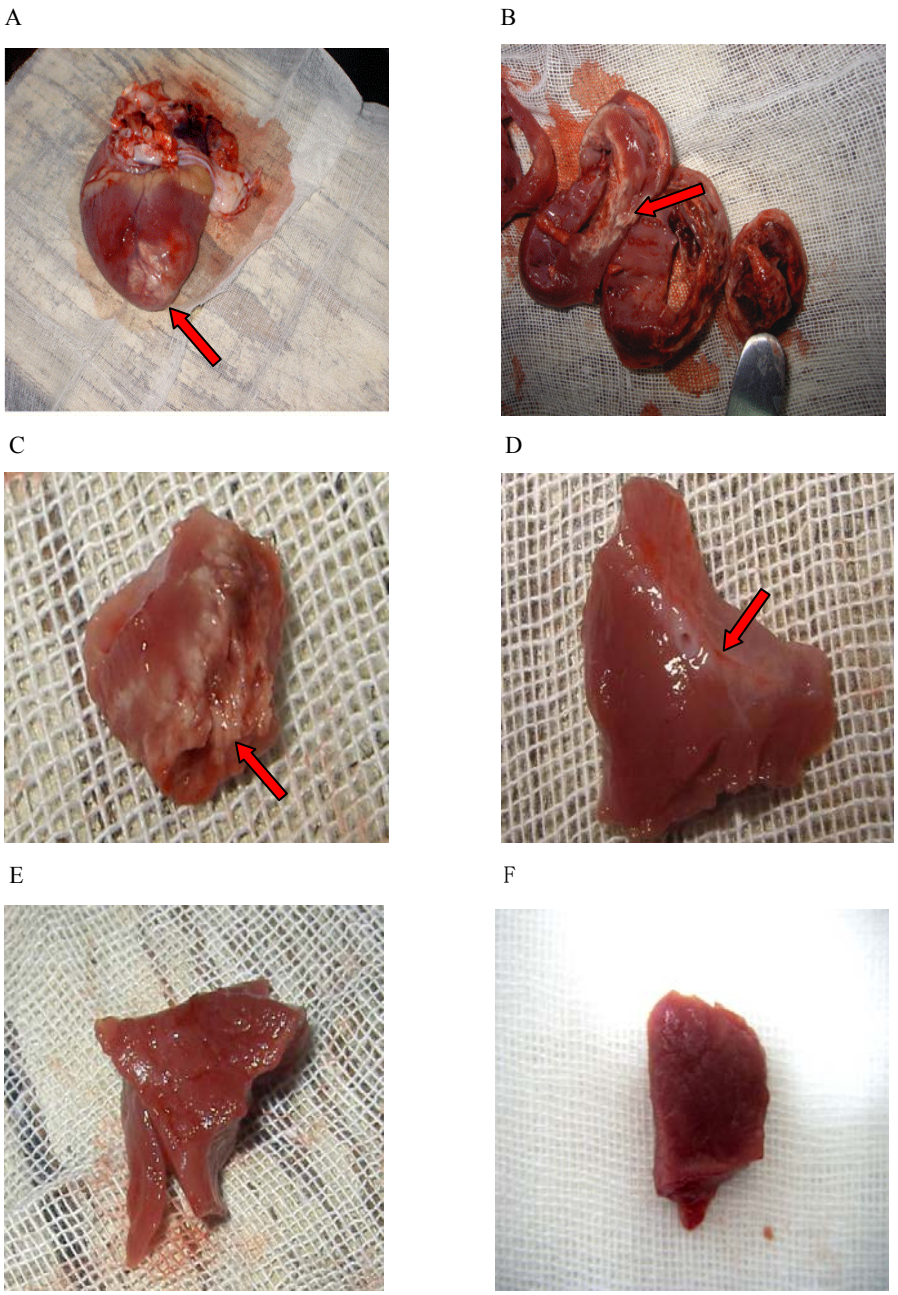

Figure 1. The myocardial biopsy specimens at 7-day of reperfused acute myocardium infarction.

Because the heart tissue specimen was taken at 7-day of reperfused acute myocardium infarction, and the infarcted myocardium (red arrow) was clearly distinguished from the non-infarcted myocardial tissue at naked eye view, thus the infarcted core was defined as the infarcted area; the periph-myocardium of the infarcted area including the infarcted myocardial tissue less than 10 percent of total crosssectional myocardial area was considered as the marginal myocardium area; the normal myocardium area indicated remote myocardium which was far away from the infarcted and marginal myocardium area and irrelevant to the distribution of occluded coronary artery blood supply. A: the heart biopsy specimens overview; B: the slices of heart biopsy specimens; C: the myocardium of infarcted area; D: the myocardium of marginal infarcted area; E: the myocardium of normal area; F: the myocardium of sham-operated area.

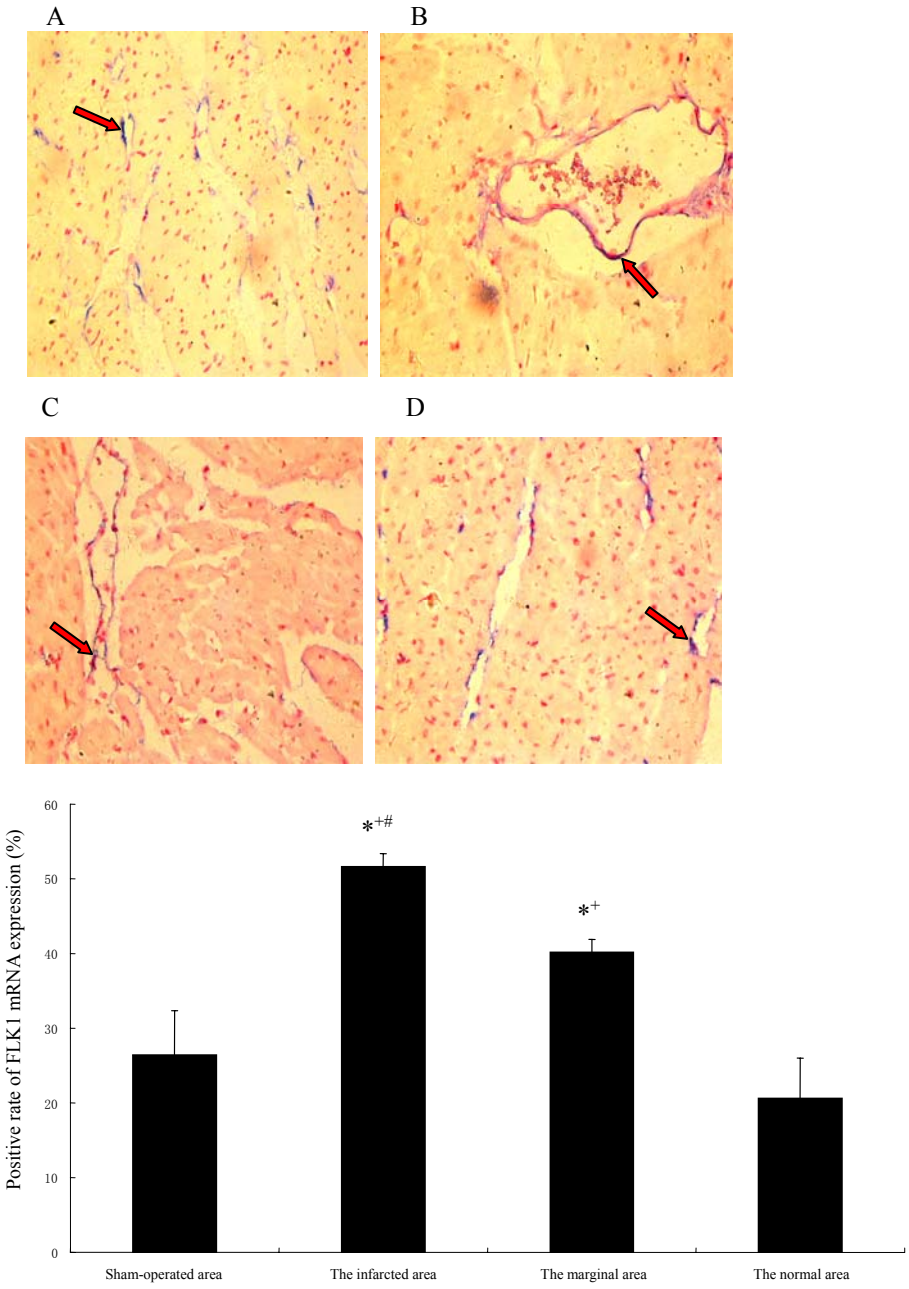

Figure 2. FLK1 positive mRNA expression in situ hybridization detection at 7-day of reperfused myocardial infarction. (light microscope,10×40)

A: the sham-operated area; B: the infarcted area; C: the marginal area; D: the normal area. The results (n=8) were presented as means ± s.e.m. *P < 0.05 vs. the sham area; $^{+}$P < 0.05 vs. the normal area; $^{\#}$P< 0.05 vs. the marginal area. FLK1 mRNA expression was stained into blue (red arrow).

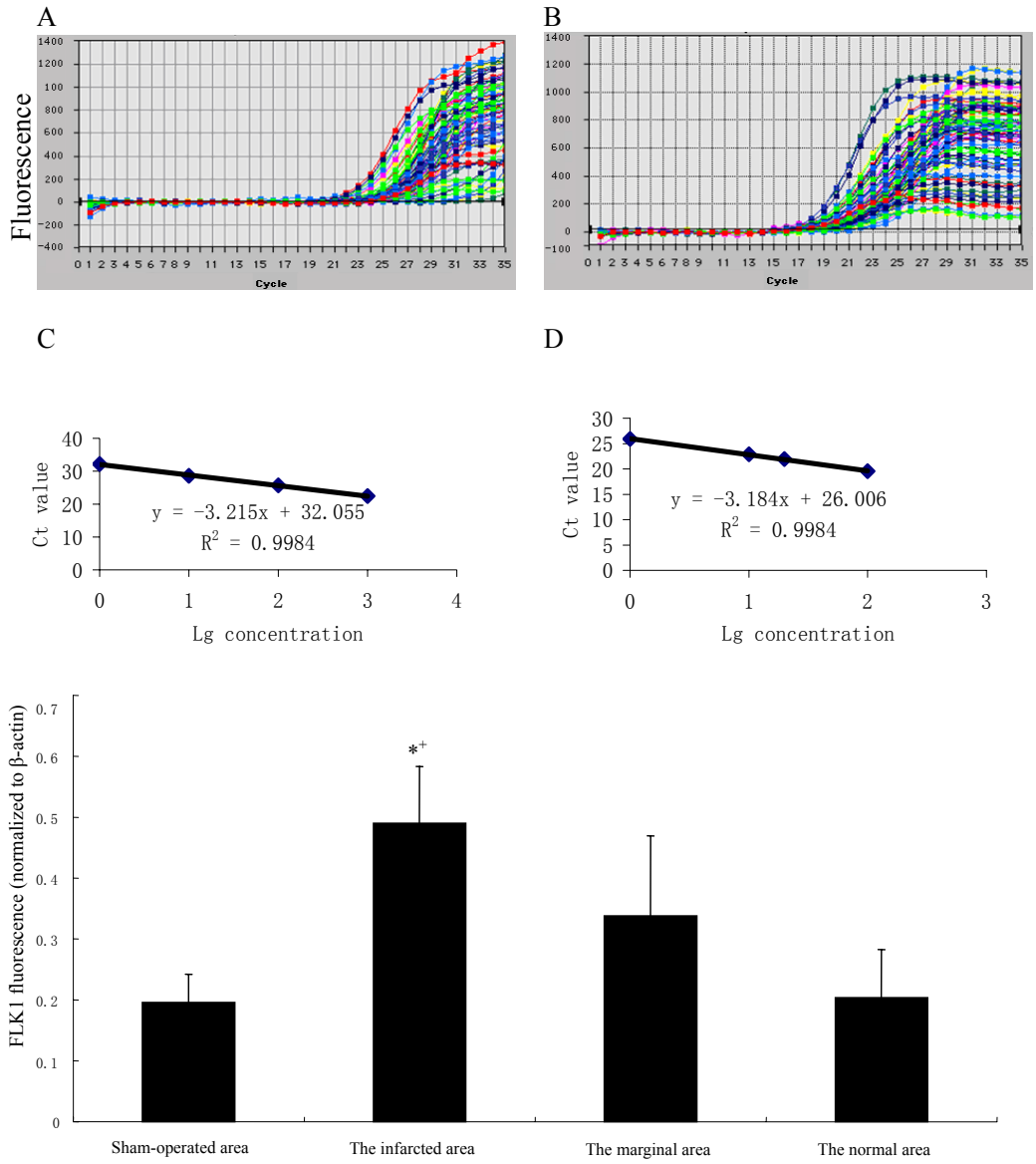

Figure 3. FLK1 mRNA expression in RQ-PCR

A and B were presented as 24 samples of quantitative fluorescence curve of β—actin and FLK1 mRNA expression in PCR cycle respectively, the y axis indicated the fluorescence signal recorded in each amplification cycle, as plotted along the x axis showed the cycle number of copies of cDNA per reaction. C and D indicated the standard curve of β—actin and FLK1 respectively, the plot shows an amplification of a limiting-dilution series of standard cDNA in vitro. The standard curve graph presented showing the relation between the logarithmic transformation of concentration in a limiting-dilution series of standard samples (on the x axis) and Ct value followed PCR cycle in the respective samples (on the y axis). The standard curve allowed quantification of cDNA in the included samples. FLK1 mRNA expression in the sham-operated area (n=6), the infarcted area (n=6), the marginal area (n=6) and the normal area (n=6) by RQ-PCR analysis. β-actin was internal control, and results (n=6) were presented as means ± s.e.m. *$P < 0.05$ vs. the sham area; $^{+}P < 0.05$ vs. the normal area; $^{\#}P < 0.05$ vs. the marginal area.

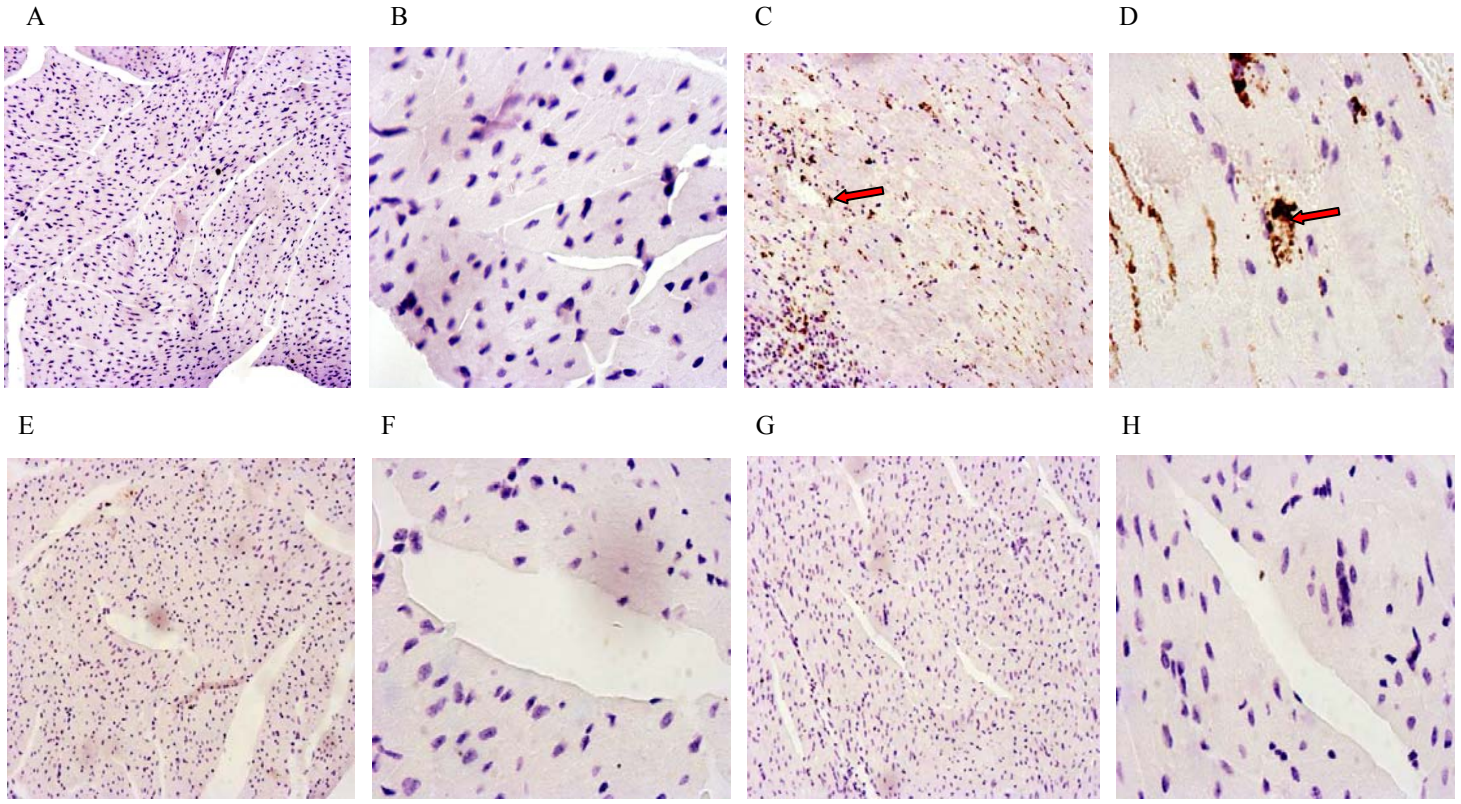

Figure 4. FLK1 protein expression in immunohistochemical staining at 7 days of reperfusion.

A: the sham-operated area (light microscope,10x10); B: the sham-operated area (light microscope,10x40); C: the infarcted area (light microscope,10x10); D: the infarcted area (light microscope,10x40); E: the marginal area (light microscope,10x10); F: the marginal area (light microscope,10x40); G: the normal area (light microscope,10x10); H: the normal area (light microscope,10x40). FLK1 protein expression was stained into brown color (red arrow).

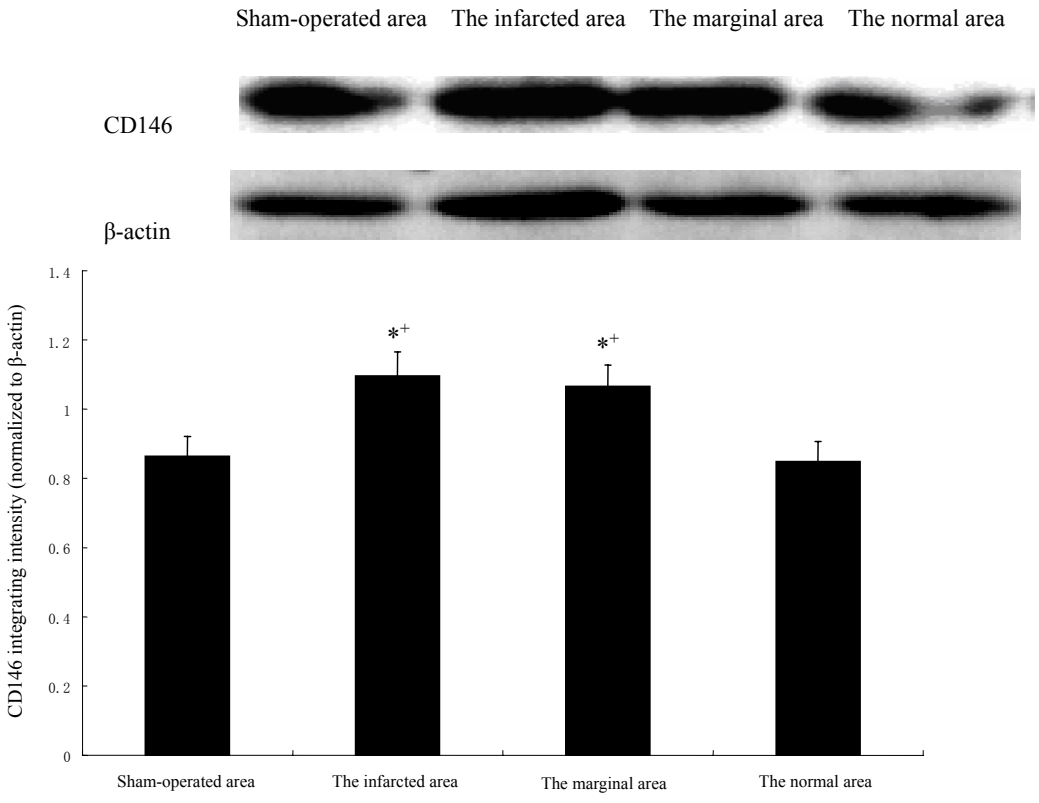

Figure 5. CD146 protein expression in heart tissue of the sham-operated group and the AMI group at 7-day of reperfused myocardial infarction.

CD146 protein expression in the sham-operated area (n=8), the infarcted area (n=8), the marginal area (n=8) and the normal area (n=8) by Western blot analysis. β-actin was internal control, and results (n=8) were presented as means ± s.e.m. *P < 0.05 vs. the sham area; $^{+}$ P < 0.05 vs. the normal area; $^{\#}$ P< 0.05 vs. the marginal area.

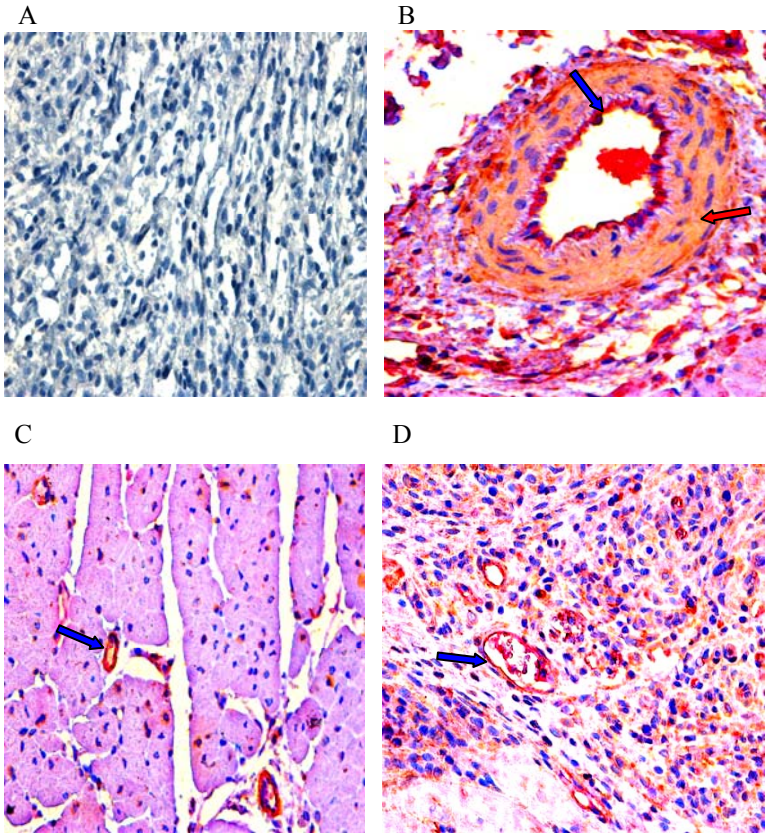

Figure 6. Microvessel density in dual immunohistochemistry stain

It combined alkaline phosphatase-based method for CD31 (red color, blue arrow) and α-smooth muscle actin immunohistochemistry with an peroxidase-based staining (brown and yellow color, red arrow). α-smooth muscle actin immunoreactivity is predominantly localized in the arteriolar media. A: negative control; B: small arteriole; C: sham-operated area; D: the infarcted area.